

A SIMULATION-BASED APPROACH TO MODELING THE UNCERTAINTY OF TWO-SUBSTRATE CLINICAL ENZYME MEASUREMENT PROCESSES

Varun Ramamohan

Research Triangle Institute - Health Solutions
300 Park Offices Drive
Durham, NC 27703, USA

James T. Abbott

Roche Diagnostics Corporation
9115 Hague Road,
PO Box 50457
Indianapolis, IN 46250-0457, USA

Yuehwern Yih

School of Industrial Engineering
Purdue University
West Lafayette, IN 47907, USA

ABSTRACT

Results of clinical laboratory tests inform every stage of the medical decision-making process, and measurement of enzymes such as alanine aminotransferase provide vital information regarding the function of organ systems such as the liver and gastrointestinal tract. Estimates of measurement uncertainty quantify the quality of the measurement process, and therefore, methods to improve the quality of the measurement process require minimizing assay uncertainty. To accomplish this, we develop a physics-based mathematical model of the alanine aminotransferase assay, with uncertainty introduced into its parameters that represent variation in the measurement process, and then use the Monte Carlo method to quantify the uncertainty associated with the model of the measurement process. Furthermore, the simulation model is used to estimate the contribution of individual sources of uncertainty as well as that of uncertainty in the calibration process to the net measurement uncertainty.

1 INTRODUCTION

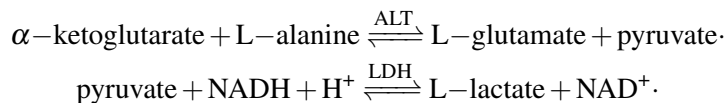
The uncertainty associated with the result of a measurement provides quantitative information regarding the quality of the measurement process. Providing this information becomes particularly important for measurements conducted in the clinical laboratory, as these measurements inform every stage of the medical decision-making process, from diagnostic and prognostic assessment of disease to determining drug dosage levels. In this article, we present a methodology for the estimation and analysis of the uncertainty associated with a class of enzyme measurement processes referred to as two-substrate enzyme assays. We illustrate the implementation of this methodology by developing a mathematical model of the uncertainty associated with the measurement of the level of activity of the alanine aminotransferase (ALT) enzyme. Uncertainty in the measurement process is represented by characterizing the parameters of the model as random variables. The Monte Carlo method is applied to estimate and analyze the uncertainty associated with the result of the measurement process.

A clinical laboratory measurement process, referred to as a clinical *assay*, consists of three stages. The first is the pre-analytical stage, which involves all activities performed before the patient sample is analyzed

on the instrument, including patient sample collection, storage, preparation prior to analysis, etc. Next is the analytical stage, which involves calibration of the instrument and subsequent analysis of the sample on the calibrated instrument. The final stage is post-analytical; and this involves recording, reporting and interpreting the result of the measurement (Burtis, Ashwood, and Bruns 2012). In this article, we restrict our attention to the analytical stage of the measurement process, since identification and characterization of the variation of the numerous sources of uncertainty associated with the pre-analytical stage requires a separate study in itself. The uncertainty associated with the post-analytical stage can largely be attributed to human error, and is beyond the scope of this study.

We model the measurement of the amount of the ALT enzyme performed on the Roche Diagnostics P-Modular Analytics measurement platform. The P-modular analytics system consists of a reaction disk with multiple reaction cells. A sampling mechanism pipettes the sample into the reaction cell and a reagent pipetting mechanism pipettes the reagents into the reaction cell. A stirrer paddle mixes the sample and the reagents to facilitate the chemical reaction, which yields a product that absorbs light passed by the photometer through the reaction cell. This quantity - the optical absorbance of the reaction mixture - is measured by the photometer. The assay itself consists of two chemical reactions, and the reactants for both reactions are supplied by two reagents. The primary reaction occurs between the substrates L-alanine (supplied by the first reagent) and α -ketoglutarate (supplied by the second reagent). The primary reaction is catalyzed by the substance to be measured - also referred to as the *analyte* - the ALT enzyme. The analyte is supplied by the patient sample, and the primary reaction yields the product of interest, pyruvate. The pyruvate reacts with the Nicotinamide adenine dinucleotide (NADH) reduced supplied by the first reagent. This reaction is catalyzed by the enzyme lactate dehydrogenase (LDH), which is also supplied by the first reagent. The rate of the primary reaction, which is directly proportional to the amount of the ALT enzyme in the patient sample, is in turn directly proportional to the rate at which NADH concentration decreases in the secondary reaction. This is explained by the fact that the rate of the secondary reaction, determined by the rate of decrease in NADH concentration, is directly proportional to the rate of formation of pyruvate, which in turn represents the rate of the primary reaction. An indicator reaction - in this case the secondary reaction, with NADH being the appropriate light-absorbing species - is required for this assay since none of the reacting species in the primary reaction absorb light at a wavelength suitable for the photometer. The NADH concentration at a given point in time is determined by the optical absorbance of the reaction mixture, and the rate of decrease in NADH concentration is determined by the rate of decrease of the optical absorbance of the reaction mixture.

The primary and secondary (indicator) reactions are given below.



A calibration function then converts the measured rate of the reaction into the “activity level” of the enzyme, which is proportional to the amount of enzyme in the patient sample. On commercial measurement platforms, the commonly used unit of enzyme activity is enzyme unit per liter (denoted as U/L), which is defined as the amount of enzyme that catalyzes the conversion of 1 micro mole of the substrate into the reaction product per minute.

The concept of measurement uncertainty and analytical rules for computing the uncertainty associated with a model of the measurement process were formalized in the Guide to the Expression of Uncertainty in Measurement (GUM), first published in 1993 (BIPM et al. 1993), and revised in subsequent editions (JCGM-100 2008). Uncertainty of measurement is defined in the GUM as “any parameter that characterizes the dispersion of the distribution of the values that can be attributed to the result of a measurement.” In this article, the parameter used is the standard deviation, since the distributions of the sources of uncertainty associated with the measurement system are modeled as Gaussian distributions, and the distribution of the measurement result is also found to be Gaussian. The quantity of the analyte to be measured, enzyme activity level, will hereafter be referred to as the *measurand*.

While there are several studies in the literature that estimate the uncertainty associated with specific clinical laboratory measurement processes (Kallner and Waldenstrom 1999, Linko et al. 2002, Sundvall et al. 2008), our search of the literature did not yield any research on the estimation of measurement uncertainty associated with the spectrophotometric determination of enzyme activity levels in general; and in particular, no studies on the estimation of the measurement uncertainty of the alanine aminotransferase enzyme assay were found. The use of a systems engineering methodology to model and estimate the uncertainty associated with clinical laboratory measurement processes has been suggested by Aronsson, de Verdier, and Groth (1974), and by Krouwer (2002). Ramamohan et al. (2012) utilize such a systems engineering perspective and build a physics-based mathematical model of the uncertainty associated with the measurement of cholesterol concentration in human blood serum, and then utilize the Monte Carlo method to perform simulation experiments to evaluate and optimize various calibration protocols in terms of minimizing the measurement uncertainty of the assay. The cholesterol assay model presented in Ramamohan et al. (2012) belongs to a class of assays known as endpoint substrate assays, wherein a single optical absorbance measurement directly quantifies the amount of cholesterol. The ALT assay model presented in this paper describes a class of significantly more complex assays, wherein the rate of the reaction is measured using multiple optical absorbance measurements, and then converted to enzyme activity level by a linear calibration function.

In this article, we use a methodology similar to that used in Ramamohan et al. (2012) and develop a mathematical model of the measurement process of the ALT assay that describes the kinetics of the catalytic process. The Monte Carlo method is then used to estimate the net uncertainty associated with the measurement system, and also to estimate the effect of uncertainty on individual components of the measurement system on the net measurement uncertainty. The use of the Monte Carlo method to estimate measurement uncertainty is appropriate if any of the following conditions apply: a.) the model of the measurement system is nonlinear; b.) the estimation of the degrees of freedom of the sources of uncertainty in the measurement system is not possible, which is the case when their variation is characterized by a non-statistical ad-hoc methodology known as Type B characterization; or c.) the distribution of the measurement result or any of the sources of uncertainty is not Gaussian (JCGM-101 2008). The first two conditions apply to the model presented in this article. The mathematical model developed, as will be shown in the following sections, is nonlinear; and the variation of the sources of uncertainty within the model is characterized by the Type B method, as opposed to statistical best-fit-to-data techniques employed in the Type A approach. Furthermore, the Monte Carlo method allows for conducting simulation experiments with the model, and therefore facilitates the extraction of information about the measurement system that would otherwise require performing controlled experiments in the laboratory.

The estimates of uncertainty obtained from the model are based on integrating performance specifications for subcomponents of the instrument into a net measurement uncertainty, and can therefore inform efforts to quantify the disparity between the expected performance of the measurement system and that observed in the clinical laboratory. The model is also used to estimate the effect of uncertainty in the individual components of the instrument and in different phases (calibration, analysis of patient sample by instrument) of the measurement process on the distribution of the measurand.

2 MODEL DEVELOPMENT

We now describe the development of the mathematical model of the uncertainty of the assay. Two reagents are added as part of the ALT assay. The first reagent, R_1 , contains the substrate L-alanine and the cofactor NADH for the primary and secondary reactions, respectively, the enzyme lactate dehydrogenase and the metal ion buffer for the reaction. The second reagent, R_2 , supplies the second substrate for the primary reaction, α -ketoglutarate. The patient sample supplies the alanine aminotransferase enzyme that catalyzes the reaction. In the following description of the model, we use the term 'substrate 1', denoted by S_1 , to refer to the L-alanine supplied by the reagent R_1 ; and the term 'substrate 2', denoted by S_2 , to the α -ketoglutarate supplied by the reagent R_2 . The volumes of the reagents R_1 and R_2 are denoted as V_{r1}

and V_{r2} . The volume of the patient sample is denoted by V_x . The concentration of a species is denoted by enclosing its symbol within square brackets. For instance, the concentrations of the substrates S_1 and S_2 in the reaction mixture will be denoted by $[S_1]$ and $[S_2]$, respectively.

The ALT activity level is directly proportional to the rate of the reaction (rate of change of absorbance with time), and is estimated using the calibration equation, specified below:

$$[E_x] = K(m_x - m_b). \quad (1)$$

Here $[E_x]$ represents the ALT activity level in the patient sample; K is the calibration parameter and m_b represents the rate of the reaction (absorbance/min) for a blank sample. The value of m_b is zero for this assay. Furthermore, any property (absorbance, activity level, volume, etc.) of the patient sample with unknown ALT activity level will be denoted using the subscript x in this article. Also, we shall henceforth refer to the measurand - the ALT activity level in the sample - as activity level in short.

K , the calibration parameter, is calculated as follows:

$$K = \frac{[E_2] - [E_1]}{m_2 - m_1}. \quad (2)$$

n absorbance measurements, recorded at equal intervals of time and denoted by A_1, A_2, \dots, A_n , are used to fit a linear relationship between absorbance and time. The rate of the reaction m is estimated by fitting a linear model between these n absorbance measurements and time, i.e.:

$$m = \frac{\sum_i t_i A_i - \frac{1}{n} \sum_i t_i \sum_i A_i}{\sum_i t_i^2 - \frac{1}{n} (\sum_i t_i)^2}. \quad (3)$$

2.1 Calibration Phase

In this phase, the value of the parameter K is established. Since the sample activity level is a linear function of the rate of change of absorbance, a two-point calibration is performed. Let $[E_1]$ and $[E_2]$ represent the desired lower and higher activity levels of the ALT enzyme in the calibrators E_1 and E_2 , respectively. Three sources of uncertainty are identified as affecting the calibrator activity level: calibrator set point uncertainty (u_{c1}), vial-to-vial variability (u_{c2}) and calibrator reconstituted stability ($u_{c3(t)}$). Calibrator set point uncertainty refers to the uncertainty in the calibrator activity level during manufacturing and prior to its use in the laboratory. Vial-to-vial variability describes the uncertainty introduced in the sample activity while preparing different vials of the calibrator supplied by the manufacturer. Finally, calibrator reconstituted stability quantifies the deterioration (percentage decrease in activity per day) of the sample when the calibrator vial is stored and reconstituted after use each day, for up to, say, N days. When these sources of calibrator uncertainty are introduced into the model, the values of $[E_1]$ and $[E_2]$ change as given below:

$$[E_1'] = [E_1] (1 + u_{c1}) (1 + u_{c2}) \prod_{t=1}^N (1 + u_{c3(t)}). \quad (4a)$$

$$[E_2'] = [E_2] (1 + u_{c1}) (1 + u_{c2}) \prod_{t=1}^N (1 + u_{c3(t)}). \quad (4b)$$

The variation of these sources of uncertainty, along with others identified as operating within the measurement process, is characterized by fitting appropriate distributions to performance specifications provided by the instrument manufacturer for each source of uncertainty. This ad-hoc non-statistical method of characterizing the variation of the sources of uncertainty is known as a Type B method, as opposed to the Type A method, which involves finding the best-fit distribution to data available for each source of uncertainty. In our case, experimental data was not available for each source of uncertainty, and hence the

use of the Type B method. As an example, specifications for vial-to-vial variability were provided by the manufacturer in the form of a coefficient of variation of 1.5%. After discussion with the manufacturer, a Gaussian distribution with a mean of 0% and a standard deviation of 1.5% was assumed to describe the variation in the calibrator activity levels due to vial-to-vial variability. The mean of the distribution was assumed to be 0%, as systematic errors in the calibrator manufacturing process were assumed to be negligible based on the manufacturer’s recommendation. Therefore, if the desired (error-free) calibrator enzyme activity level is 50 U/L, the activity level in practice would be described by a Gaussian distribution with a mean of 50 U/L and a standard deviation of 0.75 U/L.

The activity values of the calibrator are also changed due to sources of instrument uncertainty. Three sources of uncertainty are identified as operating within the instrument: sample pipetting uncertainty, reagent pipetting uncertainty and photometer uncertainty. Sample and reagent pipetting uncertainty quantify the uncertainty in the volumes of the sample and reagents that are pipetted into the reaction cell, and hence change the total volume of the reaction mixture and the number of enzyme, substrate and cofactor molecules in the reaction mixture before the reaction begins. Therefore, their effect on the assay analysis process occurs at time $t = 0$. Photometer uncertainty, however, affects each of the 15 optical measurements recorded during the reaction. These sources of uncertainty are characterized in the same way as the sources of calibrator uncertainty, and hence are also described by Gaussian distributions. The parameters of the distributions of the sources of uncertainty operating within the ALT measurement process are listed in Table 1.

Table 1: Characterization of sources of uncertainty

Source of uncertainty	Distribution	Mean (%)	SD (%)	Notes
Calibrator set point uncertainty	Gaussian	0.00	0.10	
Vial-to-vial variability	Gaussian	0.00	1.50	
Reconstituted stability	Gaussian	-1.25	0.42	Decrease in enzyme activity per day
Sample pipetting uncertainty	Gaussian	0.00	1.50	
Reagent pipetting uncertainty	Gaussian	0.00	4.00	
Photometer uncertainty	Gaussian	0.00	0.15	

We now derive the effect of sample and reagent pipetting uncertainty on each optical absorbance measurement recorded during the reaction. We first assume that the absorbance recorded at time t , denoted by A_t , is proportional to the concentration of NADH in the reaction mixture at time t (denoted by $[P_t]$). That is:

$$A_t = k[P_t] + A_{0(t)}. \tag{5}$$

Here, k is the molar extinction coefficient, $A_{0(t)}$ denotes the absorbance at time t when the pyruvate concentration at time t is zero. It is reasonable to assume that the absorbance at time t at zero pyruvate concentration is equal to the absorbance at time $t = 0$, when the pyruvate concentration is also zero. Therefore, we replace the intercept term $A_{0(t)}$ by a more general intercept term A_0 to denote absorbance of the reaction mixture at time 0 when the chemical reactions have not yet occurred, and pyruvate concentration is zero. The term A_0 is assumed to be established using a ‘reference’ method - measurement methods that are highly accurate and can be regarded as error-free for practical purposes (Tietz 1979) - and hence is assumed to be free of error. Equation 5 can then be rewritten as:

$$A_t = k[P_i] + A_0. \quad (6)$$

The initial rate of the indicator reaction is given by the rate of decrease of absorbance with time ($-\frac{dA}{dt}$), and this is in turn proportional to the initial velocity of the primary reaction. The initial rate of the primary reaction is defined by the rate of increase in concentration of pyruvate (denoted by $[P]$). At this point, we make a simplifying assumption relating the rate of decrease of the absorbance with time and the initial rate of the primary reaction as follows:

$$-\frac{dA}{dt} = \frac{d[P]}{dt}. \quad (7)$$

That is, we discard the proportionality constants and assume that the rate of decrease of absorbance is equal to the initial rate of formation of pyruvate. The initial rate of a two-substrate reaction is expressed as a function of the initial enzyme concentration, as well as the initial substrate concentrations (at time $t = 0$) (Henson and Cleland 1964). It is given by the following expression:

$$\frac{d[P]}{dt} = \frac{V_{max}}{1 + \frac{K_m(S_1)}{[S_{1(0)}}] + \frac{K_m(S_2)}{[S_{2(0)}}]}. \quad (8)$$

Here, $[P]$ denotes the concentration of the primary reaction product pyruvate at time t and V_{max} denotes the maximum reaction rate - the reaction velocity at which all the enzyme molecules are in the enzyme-substrate complex form. V_{max} can be written as the product of the turnover number k_{cat} and the initial enzyme concentration $[E_0]$ in the reaction mixture. The turnover number k_{cat} is defined as the maximum number of molecules of substrate that an enzyme can convert to product per catalytic site per unit of time. It is through this mechanism that the initial enzyme concentration influences the rate of the reaction. The terms $[S_{1(0)}]$ and $[S_{2(0)}]$ denote the L-alanine and the α -ketoglutarate concentrations, respectively, at time 0. The terms $K_m(S_1)$ and $K_m(S_2)$ are known as the Michaelis constants (Michaelis and Menten 1913, Briggs and Haldane 1925), and they denote the concentrations of the substrates at which the reaction attains half its maximum velocity while the other substrate is at its saturating concentration.

Using the assumption in equation 7, we have:

$$-\frac{dA}{dt} = \frac{k_{cat} [E_0]}{1 + \frac{K_m(S_1)}{[S_{1(0)}}] + \frac{K_m(S_2)}{[S_{2(0)}}]}. \quad (9)$$

We now use equation 9 to determine the relationship between optical absorbance of the reaction mixture and time as follows:

$$\int_{A_0}^{A_t} dA = - \int_0^t \frac{V_{max}}{1 + \frac{K_m(S_1)}{[S_{1(0)}}] + \frac{K_m(S_2)}{[S_{2(0)}}]} dt. \quad (10)$$

That is,

$$A_t = - \left(\frac{k_{cat} [E_0]}{1 + \frac{K_m(S_1)}{[S_{1(0)}}] + \frac{K_m(S_2)}{[S_{2(0)}}]} \right) t + A_0. \quad (11)$$

In order to maintain economy of notation, we express the above linear relationship between optical absorbance and time t as a function f of the initial substrate and enzyme concentrations and time t as follows:

$$A_t = - f([S_{1(0)}], [S_{2(0)}], [E_0], t) + A_0. \quad (12)$$

Now, at $t = 0$, the substrate concentrations in the reaction mixture can be written as the ratio of the number of moles of the substrates N_{S_0} to the volume of the reaction mixture V . That is, the above equation can be written as:

$$A_t = -f\left(\frac{N_{S_1(0)}}{V}, \frac{N_{S_2(0)}}{V}, [E_0], t\right) + A_0. \quad (13)$$

Furthermore, the number of moles of the substrates $N_{S_1(0)}$ and $N_{S_2(0)}$ can also be written as the product of the substrate concentrations $[S_{r1}]$ and $[S_{r2}]$ in R_1 and R_2 and their volumes V_{r1} and V_{r2} . The distinction between the terms $[S_{1(0)}]$, $[S_{2(0)}]$ and $[S_{r1}]$, $[S_{r2}]$ must be emphasized here: the first pair refers to the desired substrate concentrations in the reaction mixture at time $t = 0$, and the latter pair refers to the desired substrate concentrations in the reagents R_1 and R_2 before they are added to the reaction mixture. Therefore, the above equation can be written as:

$$A_t = -f\left(\frac{[S_{r1}] V_{r1}}{V}, \frac{[S_{r2}] V_{r2}}{V}, [E_0], t\right) + A_0. \quad (14)$$

The net volume of the reaction mixture V is the sum of the sample and reagent volumes V_s , V_{r1} and V_{r2} . We now introduce pipetting uncertainty into the model. Let the fractional change in sample volume due to sample pipetting uncertainty be x , the fractional change in reagent volumes due to reagent pipetting uncertainty be y_1 and y_2 , and the fractional change in total reaction mixture volume be denoted by z . Then,

$$V_s + \delta V_s = V_s(1 + x), \quad (15a)$$

$$V_{r1} + \delta V_{r1} = V_{r1}(1 + y_1), \quad (15b)$$

$$V_{r2} + \delta V_{r2} = V_{r2}(1 + y_2), \quad (15c)$$

$$V + \delta V = V(1 + z). \quad (15d)$$

Now, using the fact that $V = V_s + V_{r1} + V_{r2}$, we have:

$$V + \delta V = V_s(1 + x) + V_{r1}(1 + y_1) + V_{r2}(1 + y_2). \quad (16a)$$

That is,

$$\delta V = xV_s + y_1V_{r1} + y_2V_{r2}. \quad (16b)$$

Instrument uncertainty can also manifest as an error in the time at which the absorbance measurement is recorded. This can change the optical absorbance measured ostensibly at time t . This uncertainty in time of measurement is referred to as *clock uncertainty*. We denote this error in the time of measurement as δt and the fractional change in the desired time of measurement t as u_t . If we denote the change in optical absorbance measured at time t as δA_t , then the optical absorbance after the incorporation of pipetting and clock uncertainty can be written as:

$$A_t + \delta A_t = -f\left(\frac{[S_{r1}] (V_{r1} + \delta V_{r1})}{(V + \delta V)}, \frac{[S_{r2}] (V_{r2} + \delta V_{r2})}{(V + \delta V)}, [E_0], (t + \delta t)\right) + A_0. \quad (17)$$

Using equations 15a through 15d, we obtain:

$$A_t + \delta A_t = -f\left(\frac{[S_{r1}] V_{r1} (1 + y_1)}{V (1 + z)}, \frac{[S_{r2}] V_{r2} (1 + y_2)}{V (1 + z)}, [E_0], t (1 + u_t)\right) + A_0. \quad (18)$$

Subtracting equation 14 from equation 18, we arrive at the change in absorbance due to instrument uncertainty.

$$\delta A_t = \left[f \left(\frac{[S_{r1}] V_{r1}}{V}, \frac{[S_{r2}] V_{r2}}{V}, [E]_0, t \right) - f \left(\frac{[S_{r1}] V_{r1} (1 + y_1)}{V (1 + z)}, \frac{[S_{r2}] V_{r2} (1 + y_2)}{V (1 + z)}, [E_0], t (1 + u_t) \right) \right]. \quad (19)$$

We denote the fractional change in optical absorbance at time t due to pipetting and clock uncertainty, $\frac{\delta A_t}{A_t}$, by the term $u_{pc(t)}$. Now, equation 19 denotes the change in absorbance at time t from the desired value that occurs before the measurement is performed. When the measurement is performed, the uncertainty due to the photometer changes the absorbance further by the fractional amount $u_{p(t)}$. Therefore, the final expression for optical absorbance after incorporating pipetting and clock uncertainty into the model is given below:

$$A'_t = A_t (1 + u_{pc(t)}) (1 + u_{p(t)}). \quad (20)$$

The above expression denotes the value of absorbance after all sources of uncertainty affecting the optical absorbance measurement have been incorporated into the model. This process is repeated for all absorbance measurements recorded during the chemical reaction. Therefore, the corresponding rate of the reaction is estimated as follows:

$$m_{int} = \frac{\sum_i t_i A'_i - \frac{1}{n} \sum_i t_i \sum_i A'_i}{\sum_i t_i^2 - \frac{1}{n} (\sum_i t_i)^2}. \quad (21)$$

Now, since the patient sample supplies the catalyst ALT, a change in the volume of the patient sample due to sample pipetting uncertainty changes the number of enzyme molecules available for catalysis. The change in the rate of the reaction due to a change in sample volume is linearly proportional to the change in volume; that is, an $x\%$ change in the sample volume would cause the same $x\%$ change in the rate of the reaction. Therefore, the final rate of the reaction after all the sources of uncertainty operating within the calibration process is given by:

$$m' = m_{int} (1 + x). \quad (22)$$

This process of incorporating uncertainty into the calibration process is applied to both calibrators E_1 and E_2 , and their corresponding desired reaction rates m_1 and m_2 . Therefore, after incorporating the uncertainty introduced by the calibration process, this results in the estimation of the calibration factor as:

$$K' = \frac{[E'_2] - [E'_1]}{m'_2 - m'_1}. \quad (23)$$

In the case of most clinical enzyme assays, one of the calibrators is a water blank, and hence only the slope of the calibration line, the calibration factor, is estimated.

2.2 Measurement Phase

Once the calibration parameter is estimated, the process enters the measurement phase. Instrument uncertainty is the primary component of uncertainty operating within this phase.

The incorporation of instrument uncertainty into the model has been described in the previous section, and hence we denote the fractional change in optical absorbance at time t due to pipetting uncertainty and clock uncertainty in the measurement phase as $u_{pc(t,x)}$. If we denote the ‘true’ error-free enzyme activity level of the sample as $[E_x]$, and the corresponding absorbance at time t as $A_{x(t)}$, the absorbance obtained after the incorporating sample and instrument uncertainty is expressed as:

$$A'_{x(t)} = A_{x(t)} (1 + u_{pc(t,x)}) (1 + u_{p(t,x)}). \quad (24)$$

Here, A'_x represents the absorbance after the uncertainty of the measurement phase is introduced into the model. Instrument uncertainty is similarly incorporated into each absorbance measurement, and the rate of the reaction corresponding to the patient sample (denoted by $m_{int(x)}$) is estimated as the following:

$$m_{int(x)} = \frac{\sum_i t_i A'_{x(i)} - \frac{1}{n} \sum_i t_i \sum_i A'_{x(i)}}{\sum_i t_i^2 - \frac{1}{n} (\sum_i t_i)^2}. \quad (25)$$

The rate of the reaction is further changed due to sample pipetting uncertainty, as shown below:

$$m'_x = m_{int(x)} (1 + x). \quad (26)$$

The term m'_x represents the value of the rate of the reaction after all sources of uncertainty operating within the measurement process are incorporated into the model. When this value is input into the calibration line, we get the system output- the ALT activity of the sample - as:

$$[E'_x] = K' m'_x. \quad (27)$$

3 RESULTS AND ANALYSIS

The model was programmed in Python with the NumPy and SciPy packages. Clock uncertainty was not included in the implementation upon the recommendation of the manufacturer, as its magnitude is negligible in practice. Values of the rate constant k_{cat} (17100/s) and the Michaelis constants $K_{m(S_1)}$ (0.205 mmol/L) and $K_{m(S_2)}$ (5.1 mmol/L) were obtained from the BRENDA Comprehensive Enzyme Information System (Schomburg et al. 2013). Measurement uncertainties (estimated as CVs) for a range of patient sample activity levels between 10 U/L - 70 U/L varied from 1.6% - 5.5%. In order to estimate the measurement uncertainty for patient samples whose activity levels are unknown, the simulation model was used to construct an empirical function, referred to as the uncertainty profile, that generates an estimate of measurement uncertainty at a given activity level. The uncertainty profile is constructed by generating uncertainty estimates at different enzyme activity levels in the possible range of patient sample activity levels, and then finding the best-fit function to the data. The sample activity level (in U/L) is the independent variable, and the standard deviation (in U/L) of the distribution of the measurement result is the dependent variable. The uncertainty profile for the ALT assay is shown in Figure 1, and a sample activity level range of 10 U/L - 70 U/L, traversed in increments of 3 U/L, was used in constructing the uncertainty profile.

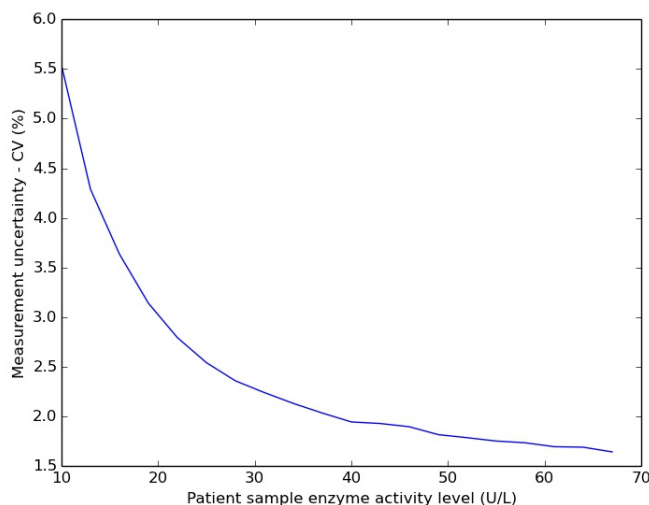


Figure 1: Uncertainty profile for alanine aminotransferase assay

A key use of such a model is to estimate the contribution of each individual source of uncertainty in both the calibration and sample analysis phase of the measurement process. The contribution of a source of

uncertainty is estimated by setting its variation to zero (mean and standard deviation of its distribution to zero), and then re-estimating the net measurement uncertainty. The absolute value of the difference between the value of the measurement uncertainty estimated without the source under consideration and the value estimated with all sources of uncertainty represents its contribution to the net measurement uncertainty.

First, we estimate the contributions of the sources of uncertainty operating within the measurement phase. The sources of instrument uncertainty operate within the measurement phase, and their individual contributions to the net measurement uncertainty are summarized in Table 2. It is clear that the photometer and the sample pipette are the largest contributors to the net measurement uncertainty, and that reducing the imprecision in their operation would lead to a substantial decrease in net measurement uncertainty. As an illustration, a decrease in 50% of photometer uncertainty (from an SD of 0.15% to 0.075%) reduces the net measurement uncertainty by approximately 14%. Similarly, a decrease of 50% in sample pipetting uncertainty (from an SD of 1.5% to 0.75%) yields a reduction of 31% in the net measurement uncertainty.

Table 2: Contribution of the sources of instrument uncertainty to net measurement uncertainty

Source	Net uncertainty with all sources operating (CV, %)	Net uncertainty with source removed (CV, %)	% Contribution to net uncertainty
Sample pipette	1.80	1.01	43.89
Reagent pipettes	1.80	1.78	1.11
Photometer	1.80	1.48	17.78

Next, the effects of the sources of calibrator uncertainty on the measurand distribution are quantified. These sources operate in the calibration phase, and hence their contribution is estimated not by studying the effect of nullifying their variation on the net measurement uncertainty, but by studying the distribution of the calibration parameter K' . The effect of these sources of uncertainty on the distribution of the calibration parameter K' is estimated by nullifying the variation of these sources of uncertainty in the calibration phase alone, and then re-estimating the net measurement uncertainty.

Uncertainty in the calibration parameter K' changes the expected value of the distribution of the measurement result. We refer to this shift in the expected value of the measurand distribution as *bias*, and we estimate the worst-case bias of the measurand due to each source of uncertainty operating within the calibration phase. We define the worst-case bias of the measurand as the absolute value of the (percentage) deviation in the expected value of the measurand distribution from the desired error-free enzyme activity level, when the calibration parameter is at ± 3 standard deviations from its expected value. Due to limitations of space, we restrict our analysis to the case when the calibration parameter is at +3 standard deviations from the mean, and refer to this worst-case bias as positive worst-case bias (denoted by WCB^+). Estimates of the worst-case bias due to each source of uncertainty are provided in Table 3.

It is evident from Table 3 that the sources of uncertainty operating within the calibration phase do not have a significant effect on the expected value of the calibration parameter. This can primarily be attributed to the fact that the expected values of the sources of uncertainty are all assumed to be zero except for reconstituted stability. Also, the sources of calibrator uncertainty, including reconstituted stability, do not have a significant effect on the distribution of K' in general. Among the sources of calibrator uncertainty, reconstituted stability has the largest effect on the worst-case bias, with a reduction of 6.72% when its variation is set to zero. It is also clear that the effects of the sources of instrument uncertainty dominate that of the sources of calibrator uncertainty on the calibration parameter, and therefore on the measurand distribution. Once again, sample pipetting uncertainty has the largest effect on the measurand distribution, with a reduction of approximately 75% in both the CV of K' , as well as the worst-case bias.

As is evident from the results above, such uncertainty models can be used to estimate the effect of the sources of uncertainty operating within both the calibration phase and the measurement phase on the distribution of the measurement result.

Table 3: Contribution of individual sources of uncertainty in the calibration phase

Source of uncertainty removed	CV of K' (%)	WCB ⁺ (%)
None	1.61	4.76
Calibrator set point uncertainty	1.54	4.60
Vial-to-vial variability	1.49	4.50
Reconstituted stability	1.51	4.44
All calibrator sources	1.52	4.48
Sample pipetting uncertainty	0.40	1.20
Reagent pipetting uncertainty	1.48	4.42
Photometer uncertainty	1.37	4.06

4 CONCLUSIONS

It was not possible to experimentally verify the model assumptions due to limitations of access to experimental equipment. However, estimates of measurement uncertainty obtained from the model were compared with uncertainty estimates provided by the instrument manufacturer. These uncertainty estimates were provided by the instrument manufacturer as an upper bound of 3.33% for the CV for ALT activity levels. As can be seen from Figure 1, this condition is satisfied for all enzyme activity levels greater than 17 U/L. Although this comparison is not an adequate substitute for experimental validation, it indicates that the model provides estimates of uncertainty comparable to laboratory estimates.

The primary aim in developing this model is to illustrate the development of mathematical models of measurement uncertainty of two-substrate enzyme assays, and their to inform laboratory practice and instrument design. In particular, we aim to demonstrate the development of mathematical models of measurement uncertainty that integrate the biochemistry of the assay with operational aspects of the assay. Such models, if accurate, will be more powerful in their prediction of assay performance than traditional statistical models.

The key advantage of developing such models lies in their use to extract information about the measurement procedure that would otherwise necessitate controlled experimentation. Furthermore, we have introduced a simulation-based method to estimate the effect of uncertainty within the calibration phase on the distribution of the calibration parameters, and consequently on the distribution of the measurement result. Finally, the use of the model to estimate the contributions of individual sources of uncertainty in both phases of the measurement process provides instrument manufacturers with guidance as to which component of the instrument should be the focus of their design efforts.

This methodology of building models of measurement uncertainty and using the models to estimate the effect of the sources of uncertainty on the measurement result can be extended to general linear, as well as nonlinear, measurement systems. The calibration function often provides a convenient starting point for developing the model of measurement uncertainty. The uncertainty in the calibration process, as has been shown in previous sections, can be incorporated into the variation in the parameters of the calibration function, and the uncertainty associated with the measurement of the sample property can be incorporated into the variation of the independent variable. After the mathematical model is developed and the sources of uncertainty are characterized, the model can be used to simulate and optimize the measurement process by determining optimal calibration protocols that minimize the net measurement uncertainty, as illustrated in Ramamohan et al. (2012).

REFERENCES

- Aronsson, T., C.-H. de Verdier, and T. Groth. 1974. "Factors Influencing the Quality of Analytical Methods: A Systems Analysis, With Use of Computer Simulation". *Clinical Chemistry* 20 (7): 738–748.

- BIPM, IEC, IFCC, ISO, IUPAC, IUPAP, and OIML. 1993. *Guide to the Expression of Uncertainty in Measurement*. Geneva: ISO.
- Briggs, G. E., and J. B. S. Haldane. 1925. "A Note on the Kinetics of Enzyme Action". *Biochemical Journal* 19 (2): 338.
- Burtis, C. A., E. R. Ashwood, and D. E. Bruns. 2012. *Tietz Textbook of Clinical Chemistry and Molecular Diagnostics*. Elsevier Health Sciences.
- Henson, C. P., and W. Cleland. 1964. "Kinetic Studies of Glutamic Oxaloacetic Transaminase Isozymes*". *Biochemistry* 3 (3): 338–345.
- JCGM-100 2008. "Evaluation of Measurement Data Guide to the Expression of Uncertainty in Measurement". Technical report, BIPM.
- JCGM-101 2008. "Evaluation of Measurement Data Supplement 1 to the "Guide to the Expression of Uncertainty in Measurement" Propagation of Distributions Using a Monte Carlo Method". Technical report, BIPM.
- Kallner, A., and J. Waldenstrom. 1999. "Does the Uncertainty of Commonly Performed Glucose Measurements Allow Identification of Individuals at High Risk for Diabetes?". *Clinical Chemistry and Laboratory Medicine* 37:907–912.
- Krouwer, J. 2002. "Setting Performance and Evaluating Total Analytical Error for Diagnostic Assays". *Clinical Chemistry and Laboratory Medicine* 48 (6): 919–927.
- Linko, S., U. Ornemark, R. Kessel, and P. D. P. Taylor. 2002. "Evaluation of Uncertainty of Measurement in Routine Analytical Chemistry Applications to Determination of the Substance Concentration of Calcium and Glucose in Serum". *Clinical Chemistry and Laboratory Medicine* 40 (4): 391–398.
- Michaelis, L., and M. L. Menten. 1913. "Die Kinetik der Invertinwirkung". *Biochem. Z* 49 (333-369): 352.
- Ramamohan, V., V. Chandrasekar, J. Abbott, G. G. Klee, and Y. Yih. 2012. "A Monte Carlo Approach to the Estimation and Analysis of Uncertainty in Clinical Laboratory Measurement Processes". *IIE Transactions on Healthcare Systems Engineering* 2 (1): 1–13.
- Schomburg, I., A. Chang, S. Placzek, C. Söhngen, M. Rother, M. Lang, C. Munaretto, S. Ulas, M. Stelzer, A. Grote et al. 2013. "BRENDA in 2013: Integrated Reactions, Kinetic Data, Enzyme Function Data, Improved Disease Classification: New Options and Contents in BRENDA". *Nucleic Acids Research* 41 (D1): D764–D772.
- Sundvall, J., T. Laatikainen, S. Hakala, J. Leiviska, and G. Alfthan. 2008. "Systematic Error of Serum Triglyceride Measurements During Three Decades and the Effect of Fasting on Serum Triglycerides in Population Studies". *Clinica Chimica Acta* 397:55–59.
- Tietz, N. 1979. "A Model for a Comprehensive Measurement System in Clinical Chemistry". *Clinical chemistry* 25 (6): 833–839.

AUTHOR BIOGRAPHIES

VARUN RAMAMOHAN is a Research Health Economist working with the Research Triangle Institute (Health Solutions) in Durham, NC. He holds a Ph.D. in Industrial Engineering from Purdue University. His email address is varun.ramamohan@gmail.com.

JAMES T. ABBOTT heads the Clinical Support Group at the Roche Diagnostics Corporation. He holds a Ph.D. in Chemistry from Queen's University (Belfast, Northern Ireland). His email address is jim.abbott@roche.com.

YUEHWERN YIH is a Professor of Production Systems in the School of Industrial Engineering at Purdue University. She holds a Ph.D. in Industrial and Systems Engineering from the University of Wisconsin at Madison. Her email address is yih@purdue.edu.